



## COMMON PATH OPTICAL COHERENCE TOMOGRAPHY USING OPTICAL CONVENTIONAL TINY PROBE IN FREQUENCY DOMAIN

SHEKHAR SRIVASTAVA<sup>1</sup>, GARIMA SAINI<sup>2</sup>

<sup>1</sup>Electronics & Communication, National Institute of Technical Teachers Training & Research (NITTTR), Panjab University, Chandigarh, India

<sup>2</sup>Assistant Professor, Electronics & Communication, National Institute of Technical Teachers Training & Research (NITTTR), Panjab University, Chandigarh, India



### ABSTRACT

Optical Coherence tomography is a dual arm imaging technique which is used to generate cross sectional or 3D view of in vivo or ex vivo of any sample which are little turbid in nature. Common path is an advanced technique of OCT which involves a single arm in set up. Ophthalmology, Endoscopy, Microscopy etc as well as in non medical stream like nondestructive evaluation of paintings and coating, online monitoring of printed electronics etc, have been using OCT techniques. CP-OCT overcomes the mismatches in OCT results by using conventional tiny probe and image can be reconstructed with less errors.

Keywords— Common Path Optical coherence Tomography, CPOCT, FD-OCT, OCT imaging.

©KY Publications

### I. INTRODUCTION

OCT is a non-contact and harmless imaging technique. It is analogous to ultrasound. It works in the range of near infrared. It works in both time domain and in frequency domain. Basic set up of dual arm time domain OCT is shown in Fig. 1.

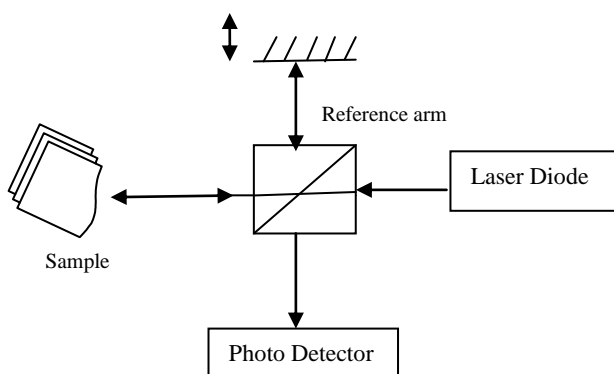


Fig.1 Dual Arm OCT set up

Time delay between reflected light is measured to determine depth of the reflecting structure. Due to the short time delays between signals OCT must use an interferometer to detect the reflected light. Interference fringes are formed when the sample and reference arms are within a small range. A depth profile is formed by the detection of the interference pattern between the reference and sample arm as the reference arm is scanned. This is called A-scan. Taking lateral scans on various x-positions by moving the used probe tip, it gives the B-scan which is then converted in a cross sectional image by some image processing. The operating principle is based on low coherence spectral interferometry [1]. The total optical signal reflected back from a sample consists of multiple arbitrary waves reflecting from interfaces at different depth  $z$ . This signal interferes with the reference wave continuous reflecting from the inner surface area of the tip as reflection resulting in spectral fringes Fig. 2 of constructive and destructive interference.

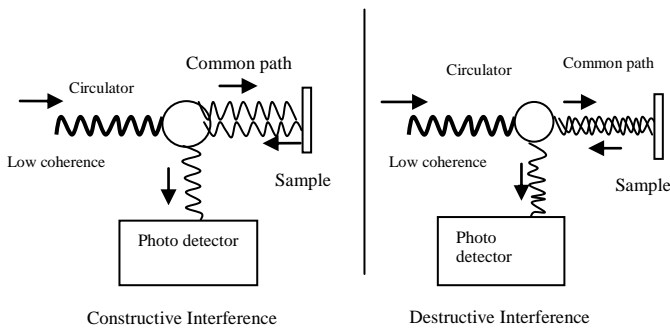


Fig. 2 Interference process in OCT

The advantage of this spectral approach (Frequency domain) is that the full structure signal is obtained in a single measurement and no depth scanning is required. The interference signal  $I(k)$  can be described by [2]:

$$\begin{aligned}
 I_D(k) = & \frac{\rho}{4} [S(k)[R_R + R_{S1} + R_{S2} + \dots]] \dots \text{1st term} \\
 & + \frac{\rho}{2} [S(k) \sum_{n=1}^N \sqrt{R_R R_{S_n}} (\cos[2kn(z_R - z_{S_n})])] \dots \text{2nd term} \\
 & + \frac{\rho}{4} [S(k) \sum_{n \neq m=1}^N \sqrt{R_{S_n} R_{S_m}} (\cos[2kn(z_{S_n} - z_{S_m})])] \dots \text{3rd term} \\
 & \dots \text{Eq. (1)}
 \end{aligned}$$

Where we have neglected the phase of the reflectivity coefficients. Here,  $2z$  is the path length difference between the sample arm and the reference plane,  $R_R$  is the power reflectivity of the reference reflector (fiber tip),  $R_{S_n}$  or  $R_{S_m}$  is power reflectivity of multiple layers of sample, where  $n \neq m = 1$ ,  $S(k)$  is the spectral intensity distribution of the light source,  $n$  is the refractive index of the sample and  $\rho$  is the responsivity of the detector.

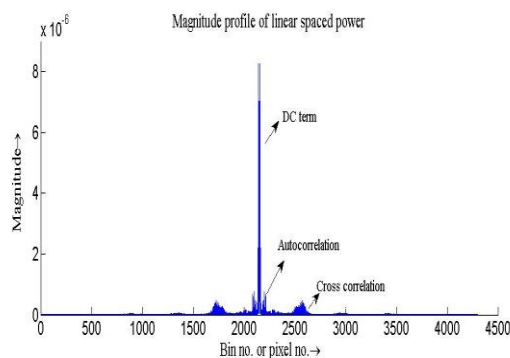


Fig. 3 Magnitude profile after IFFT of acquired intensity spectrum

From Eq. (1), the total interference signal is a superposition of three terms as shown in fig. 2. The first term is a path length-independent offset to the detector current, scaled by the light source wave number spectrum and with amplitude proportional

to the power reflectivity of the reference mirror plus the sum of the sample reflectivities. This term is often referred to as “constant” or “DC” component. This is the largest component of the detector current if the reference reflectivity dominates the sample reflectivity.

The second term describes the depth information of the sample. A “cross-correlation” component for each sample reflector, which depends upon both light source wave number and the path length difference between the reference arm and sample reflectors. This is the desired component for OCT imaging. Since these components are proportional to the square root of the sample reflectivity, they are typically smaller than the DC component. However, the square root dependence represents an important logarithmic gain factor over direct detection of sample reflections [2].

The third term describes the mutual interference of all elementary waves and may be neglected in most cases of strongly scattering medium. “Autocorrelation” terms representing interference occurring between the different sample reflectors appear as artifacts in typical OCT system designs (exceptions occur in common-path system designs, in which the autocorrelation component represents the desired signal). Since the autocorrelation terms depend linearly upon the power reflectivity of the sample reflections, a primary tool for decreasing autocorrelation artifacts is selection of the proper reference reflectivity so that the autocorrelation terms are small compared to the DC and interferometric terms [2-5].

The inverse Fourier transform of  $I(k)$  makes it possible to distinguish between these terms. The first term corresponds to the correlogram of the light source which can be filtered out while the third term gives the ranging information of scattering amplitude at different reflecting interface locations from which a cross-section tomogram of the sample can be constructed [6].

## II. CP-OCT SYSTEM

Due to presence of dual arm there are some mismatches in the set up and in results too. Mismatches are like dispersion, polarization and temperature which blurred the image or decrease

the axial resolution [7]. Common path is a technique of OCT in which only single arm is used instead of dual arm by removing dynamic mirror with the mirror in the sample arm or just taking a special kind of probe. A mirror is placed in front of sample and reflected light is collected at the used probe tip. This works as reference light. Whether in the special type of tiny tip probe the reference light is obtained from the reflection of inner surface of tip of the probe. In this way reference light can be obtained in single arm whatever is obtained from dual arm [8]. This will reduce the length of optical fiber and this reduced length can be used to increase the length in sample arm to reach nearer to the object like small tissues of body. CPOCT improves the sensitivity to vibrations and increase the scanning speed, simplicity and robustness [9].

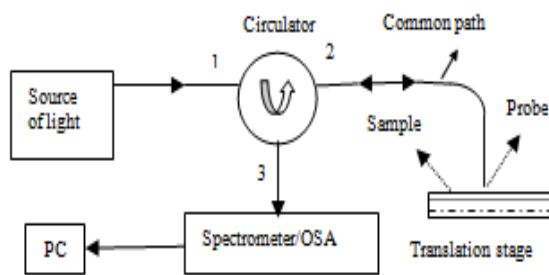


Fig. 4 CPOCT set up

### III. TINY TIP OF CONVENTIONAL PROBE USED IN THE EXPERIMENT

In this section, the chemical fabrication process of the conical micro tip and the implementation of the in fiber common-path technique within a Fourier-domain OCT system is briefed. A hydrofluoric (HF) etching solution is used in the selective-chemical etching technique. The physical process involved in this selective-chemical etching process is a simple process which only requires immersion of a single mode fiber into the HF solution. In our experiments, we used Corning single mode fiber, which has a core diameter of  $8\mu\text{m}$ , cladding diameter  $125\mu\text{m}$  and a cut-off wavelength at  $1547.50\text{nm}$ .

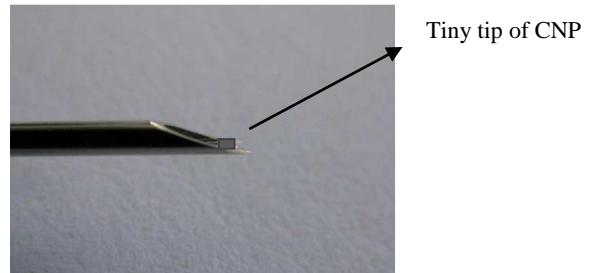


Fig. 5 Conventional tiny probe tip

### IV. EXPERIMENTAL SET UP

The experimental diagram of the common-path FD-OCT setup is shown in Fig. 4. The low coherence light source is a super luminescent diode (SLD) with a centre wavelength of  $1547.50\text{nm}$  and spectra width of  $28\text{nm}$ . A circulator is used instead of a  $2\times 2$  coupler because no additional arm is required. A commercial OSA (Yokogawa AQ6370D) which incorporates a single detector with rotating grating (The measured dynamic range of the system is approximately  $78\text{dB}$ ). The optical power, from the tiny-tip fiber probe, incident on the sample was measured using a photo-detector (PDA10CS, Thorlabs Inc.) to be approximately  $5\text{mW}$ . The motorized translation stage (KT-LS13-M, Zaber Technologies Inc.) provides the lateral scanning for the B-scan operation. A custom program was written with MATLAB vR2010 to operate and collect data from this experimental CPOCT system.

### V. IMAGE PROCESSING

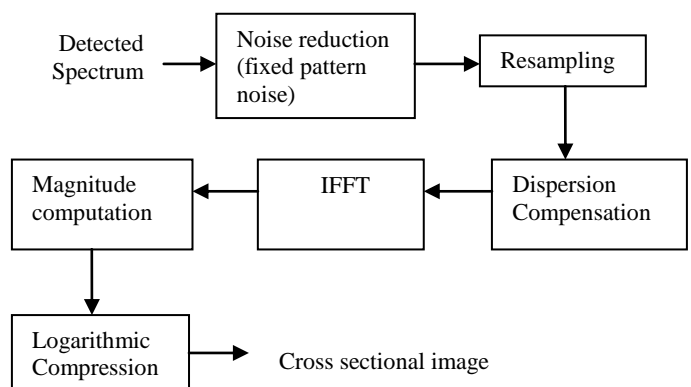


Fig. 6 Block diagram of Image construction  
 Image generation involves signal and image processing steps [10-11] mentioned in as in above block diagram. This all work has been done through MATLAB v R2010 by making programs.

## VI. RESULT: Cross Sectional Image

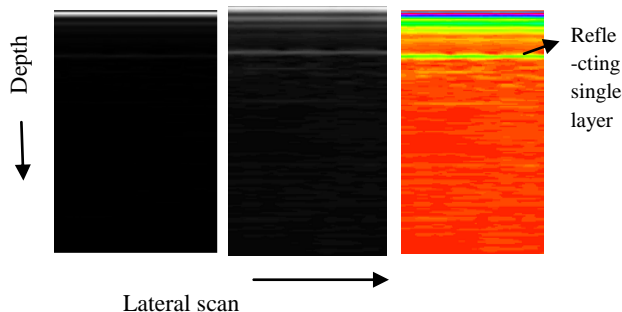


Fig. 7 Cross section image of mirror single layer

Above fig. shows images of a single reflecting layer of a mirror inner part which is generated by following an image processing techniques. Initial obtained result (left) is showing a light single line which is then more visible by enhancing contrast of the image (middle) and color map –hot (right). This single line is reflecting surface of the mirror. We can also get the depth of this reflecting layer.

## VII. CONCLUSION

From the initial obtained results it can be demonstrated that this CPOCT with conventional tiny probe techniques can be very useful for in vivo and ex vivo imaging applications. This will enhance the visualization and generate good images which can be very useful in clinical applications. Future work is to replace the probe with some enhanced quality of tip that may generate small spot size and high penetrating light which may enhance the image quality.

## REFERENCES

- [1] Liu B, Brezinski ME, "Theoretical and practical considerations on detection performance of time domain, fourier domain, and swept source optical coherence tomography", Journal of Biomedical Optics, Vol. 12, No.4, pp: 7-12, 2007.
- [2] J.A. Izatt and M.A. Choma, "Theory of Optical Coherence Tomography". Book Title- Optical Coherence Tomography, Springer Link, pp: 47-72, 2008.
- [3] P.H. Tomlins and R.K. Wang, *Theory, Developments and Applications of Optical Coherence Tomography*, Journal of Physics D: Applied Physics, pp. 2519 - 2535, Vol. 38, Jul. 2005.
- [4] W. Drexler, "Ultra-high-resolution optical coherence tomography," J. Biomed. Opt. Vol.9, pp: 47-74, 2004.
- [5] A. R. Tumlinson, B. Považay, L. P. Hariri, J. McNally, A. Unterhuber, B. Hermann, H. Sartmann, W. Drexler, and J. K. Barton, "In vivo ultra-high-resolution optical coherence tomography of mouse colon with an achromatized endoscope," J. Biomed. Opt., Vol. 11, (2006).
- [6] S. Chandra Sekhar, Rainer A. Leitgeb, Adrian H. Bachmann, and Michael Unser, "Logarithmic Transformation technique for exact signal recovery in frequency-domain Optical-Coherence Tomography", SPIE-OSA, Vol. 6627, No.14, pp:1-6, 2007.
- [7] Andrei B. Vakhtin, Daniel J. Kane, William R. Wood, and K. A. Peterson, "Common-path interferometer for frequency-domain optical coherence tomography," Appl. Opt. Vol. 42, pp: 6953-6958, 2003
- [8] A. Popp, M. Wendel, L. Knels, P. Knuschke, M. Mehner, T. Koch, D. Boller, P. Koch, and E. Koch, "Common-path Fourier domain optical coherence tomography of irradiated human skin and ventilated isolated rabbit lungs," Proc. of SPIE-OSA Biomedical Optics 5861 2005.
- [9] U. Sharma, and J. U. Kang, "Common-path optical coherence tomography with side-viewing bare fiber probe for endoscopic optical coherence tomography," Rev. Sci. Instrum., Vol. 78, 113102, 2007
- [10] Murtaza Ali and Renuka Parlapalli, "Signal Processing Overview of Optical Coherence Tomography Systems for Medical Imaging", Texas Instrument, White Paper SPRABB9, 2010.
- [11] Hamid Hossieny and Carla Carmelo Rosa, "Numerical Study on Spectral Domain Optical Coherence Tomography Spectral Calibration and Re-Sampling Importance", Photonic Sensors, Vol. 3, No.1, pp: 35-43, 2013.